Dynamics of Solar and Stellar Convection Zones and Atmospheres
Proceedings IAU Symposium No. 365, 2024
A. V. Getling & L. L. Kitchatinov, eds.
doi:10.1017/S1743921323004982

Dominating active regions in the minima of solar activity

R. A. Suleymanova and V. I. Abramenko

Crimean Astrophysical Observatory of Russian Academy of Sciences, Nauchny, Russia
email: bictr97@gmail.com

Abstract. During minima of solar activity, it is possible to estimate the influence of convection zone turbulence on the magnetic flux tubes forming active regions (ARs), because the toroidal field of the old cycle weakens, and the new toroidal field is still weak. We analyzed ARs of solar minima between 23-24 and 24-25 solar cycles. ARs were classified as regular, irregular and unipolar spots. Regular ARs follow the empirical laws consistent with the Babcock–Leighton dynamo theory. We found that regular ARs dominate by flux and by number during the solar minima. Irregular ARs are mainly represented by bipolar structures of deformed orientation and contribute only one-third in the total flux and one-third in the total number. Very complex multipolar ARs are extremely rare. So, during solar minima the global dynamo still guides the formation of ARs, whereas the turbulence only slightly affects the toroidal flux tubes orientation.

Keywords. Sun:magnetic fields, Sun:active regions, Sun:solar cycle

1. Introduction

According to Babcock–Leighton dynamo theory Babcock (1961), Leighton (1969) the solar activity is cyclic: in the maximum phase there are strong toroidal filed, increased number of active regions (ARs) and flares, whereas in the minimum there is strong poloidal field, the toroidal field of the previous cycle ceased and the new toroidal field is still weak. At the same time the turbulence in the convection zone works with the same intensity through all of these periods, so at the minima of solar activity the manifestation of turbulence on the AR formation might be the most pronounced. The aim of our work is to clear up what component of solar dynamo is the most effective in the minima of solar activity: global dynamo or turbulent component of dynamo.

2. Data and methods

We considered two periods: from January, 2008 till June, 2009 (the deep minimum between cycles 23rd-24th) and from April, 2018 till April, 2020 (the deep minimum between cycles 24th-25th). These intervals were chosen according to the curve of the total sunspot area variations presented at Abramenko *et al.* (2023) and obtained from the monthly average sunspot area data (http://solarcyclescience.com/AR_Database/sunspot_area.txt). The curve is marked with dash-dotted line and intervals are marked with vertical dotted lines in Fig. 1 and 2.

For 23rd cycle we used line-of-sight (LOS) magnetograms in Ni I 6768 $\AA$ line with a spatial resolution of 4 arcsec acquired by Michelson Doppler Imager (MDI) on board the Solar and Heliospheric Observatory (SOHO) Scherrer *et al.* (1995). For 24th cycle we used LOS magnetograms (Space-weather HMI Active Region Patches, SHARP, sharp_cea_720s) in Fe I 6173.3 $\AA$ line with the spatial resolution of 1 arcsec acquired by Helioseismic and Magnetic Imager (HMI) on board the Solar Dynamics Observatory (SDO) Scherrer *et al.*

Table 1. The ARs during solar minima 23rd-24th, 24th-25th (beginning of the table).

NOAA	Date of observation	Coordinates (latitude; longitude)	Magnetic flux, 10^{21} Mx	HJL	MMC class	MW class
10982	2008.01.31	-8.39; -35.37	11.0	YYN	B1	β
10983	2008.02.26	-5.29; 42.41	2.4	YYN	B1	α
10987	2008.03.27	-7.60; -3.88	14.3	YYY	A1	β
10988	2008.03.271	-7.61; -28.10	15.1	YYY	A1	β
10989	2008.03.28	-11.00; -46.44	9.8	Y0P	U	β
10992	2008.04.23	12.25; 5.72	2.4	YNY	B1	β

(2012), Schou *et al.* (2012). To retrieve the data we used the website of the Joint Science Operations Center (JSOC, http://jsoc.stanford.edu/).

Each AR located closer than 60° from the disc center and having the unsigned magnetic flux above 10^{21} Mx was counted once at the moment of its maximum development. This way, we found 21 ARs during the first minimum and 41 ARs during the second minimum.

To distinguish between the global dynamo action and the turbulent component of the dynamo, we need to classify each AR in the framework of the magneto-morphological classification (MMC), described in Abramenko *et al.* (2018), Abramenko (2021), Abramenko *et al.* (2023). In brief, the regular ARs produced by the global dynamo are classified as A-class. They follow the empirical lows of the mean-field dynamo theory, in particular, the Hale polarity law, the Joy's law, the prevalence of the leading spot Babcock (1961), van Driel–Gesztelyi & Green (2015). All the rest, except unipolar spots, are the ARs violating the empirical laws and therefore might be considered as disturbed by turbulence in the convection zone. The degree of disturbance is reflected in the complexity of the ARs which increases from B1, to B2, to B3 class.

In this manner, we classified all 62 ARs. Results are collected in the table, the beginning of which is shown in Table 1. Except for the common parameters in the four columns (NOAA number, date of observation, coordinates, total magnetic flux), the column 5 represents the perfection of the empirical laws: YES (Y) or NO (N) in the following order: Hale law, Joy's law, the leading sunspot prevalence. The next two columns show the AR class: according to MMC and to the Mount Wilson classification Hale et al. (1919). Out of all 62 ARs, 52 turned to belong to the β class by Hale classification. So, we don't get much for our purposes of the dynamo diagnostics, therefore below we considered only the MMC class.

3. The ARs distributions during the minima of solar activity

Fig. 1 represents how ARs are distributed in the time-flux diagram during to minima 23rd-24th (panel a) and 24th-25th (panel b). The dash-dotted line shows the average monthly sunspot areas smoothed over an interval of 13 months, and dashed vertical lines show the accepted boundaries of the deep cycle minimum. Regular ARs are represented by blue color: asterics for A1 class, straight crosses for A2 class. Red symbols show irregular ARs: filled circles for B1 class, open circles for B2 class. Green rhombuses show the unipolar sunspots.

The comparison of distribution of regular ARs (top panels) with that for irregular ARs (bottom panels) is shown in Fig. 2. During each minimum the number of regular ARs more than twice exceeds the number of irregular. So, the toroidal field of the global dynamo steel prevails the turbulent convection in generation of ARs. Out of the total number of 18 irregular ARs during both minima 15 of them are wrong bipolar structures of B1 class, so the influence of the turbulence is rather mild during the minimum. It is also interesting to note that there are only 3 ARs of B2 class and none of ARs of the most complex B3 class.

https://doi.org/10.1017/S1743921323004982 Published online by Cambridge University Press

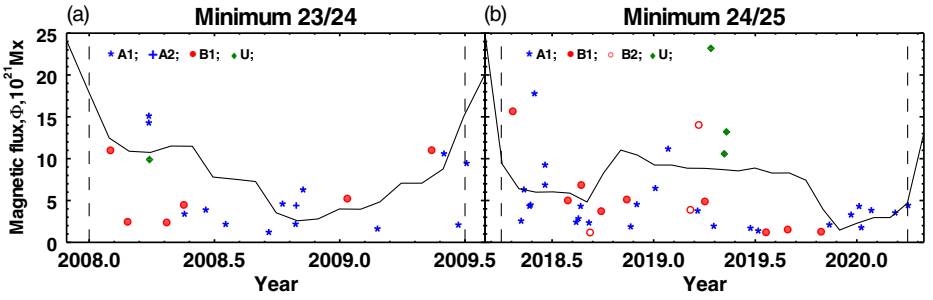

Figure 1. Occurrance of ARs during 2 solar minima: blue symbols represent regular ARs (asterics for A1 class, straight crosses for A2 class), red symbols represent irregular ARs (filled circles for B1 class, open circles for B2 class). Filled green rhombuses represent the unipolar sunspots. The dash-dotted line and dashed vertical lines show the average mounthly sunspot areas and selected time interval respectively.

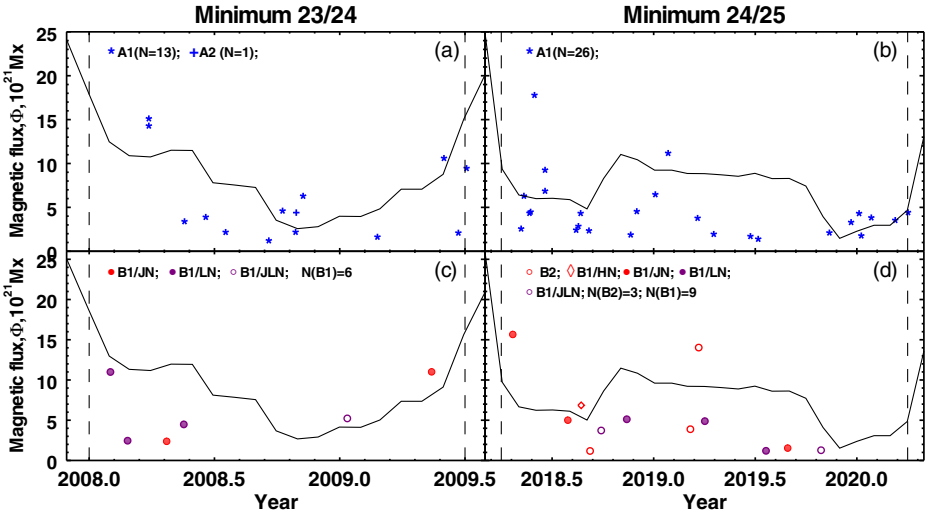

Figure 2. A separate representation of regular and irregular ARs occurrance during 2 solar minima. The designations of A1, A2 and B1 classes coinside with designations in Fig. 1. Red rhombuses represent ARs of B1 class with Hale's law violation (B1/HN). ARs with wrong Joy's law violation are represented by filled red circles (B1/JN). Purple filled circles are represent ARs with violation the rule of dominance of the leader spot (B1/LN). Open purple circles show the ARs that not obey the Joy's law and the rule of dominance of the lider spot (B1/JLN). Other notations are the same as in Fig. 1.

It can be noticed that for the entire considered intervals, regular ARs dominate over irregular ones. Consequently, both the previous toroidal field of old cycle and the new toroidal field of the oncoming cycle work against the background of weak fluctuations caused by turbulence. It could be concluded that turbulence by itself cannot cause a large flow, since it can only distort the existing flow.

The composition of the summed flux from all ARs (gray bars) during minima (top panels) and maxima (bottom panels) is presented in Fig. 3. We see that the total flux from regular ARs dominates twice the total flux of irregular ARs. However, during the maxima, the total flux of regular ARs is approximately equal to the summed flux from all irregular ARs. In other words, during minima the global dynamo dominates in ARs production whereas during the maxima about half of total ARs flux is distorted by turbulence.

https://doi.org/10.1017/S1743921323004982 Published online by Cambridge University Press

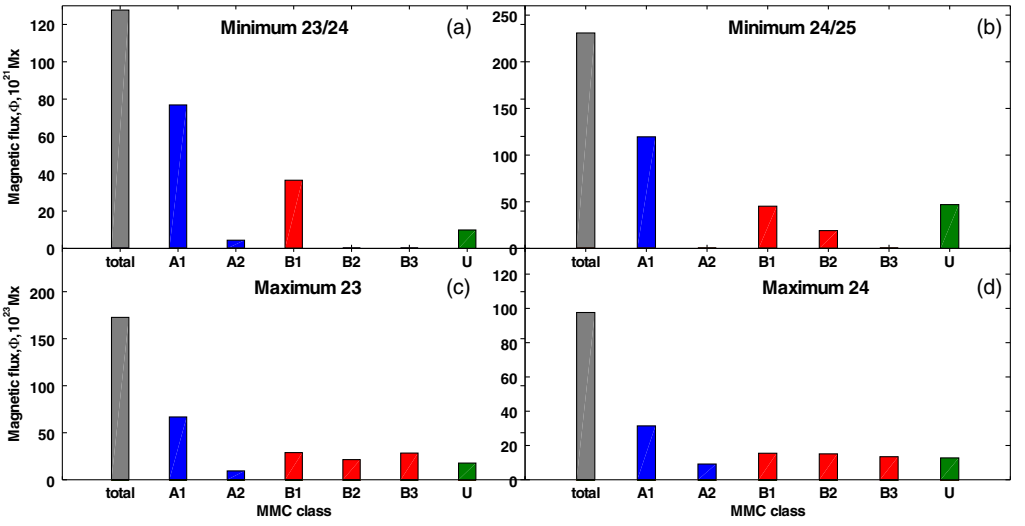

Figure 3. A histogram of ARs over different classes. Upper row, data on two minima studied in this work; bottom row - data for the 23rd cycle maximum, and for the 24th cycle maximum. The vertical scales differ by two orders of magnitude.

4. Conclusions

The following conclusions can be drawn:

- Regular ARs were observed twice more frequently than irregular ARs.
- The summed flux from regular ARs was twice higher than that from irregular ARs.
- The simplest bipolar structures of A1 and B1 classes consist of 87% from all observed ARs.
- During solar minima the magnetic flux from ARs is still dominated by the toroidal flux of global dynamo with very mild influence from the turbulent component of the dynamo.

Acknowledgments

SDO/HMI data is available through the SDO/HMI and SDO/AIA Science Groups. SDO is NASA's Living With a Star (LWS) mission. SOHO/MDI data is available through the SOHO/MDI and SOHO/EIT Science Groups. SOHO is an international collaboration between ESA and NASA. The SDO/HMI and SOHO/MDI data were provided by the Joint Science Operation Center (JSOC).

References

Abramenko, V.I. 2021, *MNRAS*, 507, 3698.
Abramenko, V.I., Suleymanova, R.A., Zhukova, A.V. 2023, *MNRAS*,518,, 4746.
Abramenko, V.I., Zhukova, A.V., Kutsenko, A.S. 2018, *G&A*,58, 1159.
Babcock, H.W. 1961, *A&A*, 133, 572.
Hale, G.E., Ellerman, F., Nicholson, S.B., *et. al* 1919, *ApJ*,49, 153.
Leighton, R.B. 1969, *ApJ*, 156, 1.
Scherrer, P.H., Bogart, R.S., Bush, R.I.,, *et al.* 1995, *SoPh*,162, 129.
Scherrer, P.H., Schou, J., Bush, R.I.,, *et al.* 2012, *SoPh*,275, 207.
Schou, J., Scherrer, P.H., Bush, R.I.,, *et al.* 2012, *SoPh*,275, 229.
van Driel–Gesztelyi, L., Green, L.M. 2015, *LRSP*,12, 1.

https://doi.org/10.1017/S1743921323004982 Published online by Cambridge University Press